Feasibility of using deep learning to detect coronary artery disease based on facial photo

Shen Lin[1†], **Zhigang Li** [2†], **Bowen Fu**[2†], **Sipeng Chen**[3], **Xi Li**[1], **Yang Wang**[4], **Xiaoyi Wang**[1], **Bin Lv**[1,5], **Bo Xu** [1,6], **Xiantao Song**[7], **Yao-Jun Zhang** [8], **Xiang Cheng** [9], **Weijian Huang**[10], **Jun Pu**[11], **Qi Zhang**[12], **Yunlong Xia** [13], **Bai Du**[14], **Xiangyang Ji**[2*], and **Zhe Zheng** [1,15,16*]

[1]National Clinical Research Center of Cardiovascular Diseases, State Key Laboratory of Cardiovascular Disease, Fuwai Hospital, National Center for Cardiovascular Diseases, Chinese Academy of Medical Sciences and Peking Union Medical College, No. 167 Beilishi Road, Xicheng District, Beijing 100037, People's Republic of China; [2]Department of Automation, Tsinghua University, Main building, Haidian District, Beijing 100084, People's Republic of China; [3]Department of Information Center, Fuwai Hospital, National Center for Cardiovascular Diseases, Chinese Academy of Medical Sciences and Peking Union Medical College, No. 167 Beilishi Road, Xicheng District, Beijing 100037, People's Republic of China; [4]Medical Research & Biometrics Center, Fuwai Hospital, National Center for Cardiovascular Diseases, Chinese Academy of Medical Sciences and Peking Union Medical College, No. 167 Beilishi Road, Xicheng District, Beijing 100037, People's Republic of China; [5]Department of Radiology, Fuwai Hospital, National Center for Cardiovascular Diseases, Chinese Academy of Medical Sciences and Peking Union Medical College, No. 167 Beilishi Road, Xicheng District, Beijing 100037, People's Republic of China; [6]Department of Cardiology, Fuwai Hospital, National Center for Cardiovascular Diseases, Chinese Academy of Medical Sciences and Peking Union Medical College, No. 167 Beilishi Road, Xicheng District, Beijing 100037, People's Republic of China; [7]Department of Cardiology, Beijing Anzhen Hospital, Capital Medical University, No. 2 Anzhen Road, Chaoyang District, Beijing 100029, People's Republic of China; [8]Department of Cardiology, Xuzhou Third People's Hospital, Xuzhou Medical University, No. 131 Huancheng Road, Huaihai Economy District, Xuzhou 221000, People's Republic of China; [9]Department of Cardiology, Wuhan Union Hospital, No. 1277 Jiefang Avenue, Jianghan District, Wuhan 430022, Hubei, People's Republic of China; [10]Department of Cardiology, The First Affiliated Hospital of Wenzhou Medical University, Nanbaixiang Road, Ouhai District, Wenzhou 325000, People's Republic of China; [11]Department of Cardiology, RenJi Hospital, Shanghai JiaoTong University Medical College, No. 160 Pujian Road, Pudong New District, Shanghai 200120, People's Republic of China; [12]Department of Cardiology, Shanghai East Hospital, Tongji University School of Medicine, No. 150 Jimo Road, Pudong New District, Shanghai 200120, People's Republic of China; [13]Department of Cardiology, The First Affiliated Hospital of Dalian Medical University, No. 222 Zhongshan Road, Xigang District, Dalian 116011, People's Republic of China; [14]Department of Cardiology, Guang'anmen Hospital, China Academy of Chinese Medical Sciences, No.5 Beixiange Road, Xicheng District, Beijing 100053, People's Republic of China; [15]Department of Cardiovascular Surgery, Fuwai Hospital, National Center for Cardiovascular Diseases, Chinese Academy of Medical Sciences and Peking Union Medical College, No. 167 Beilishi Road, Xicheng District, Beijing 100037, People's Republic of China; and [16]National Health Commission Key Laboratory of Cardiovascular Regenerative Medicine, Fuwai Central-China Hospital, Central-China Branch of National Center for Cardiovascular Diseases, No.1 Fuwai Avenue, Zhengdong New District, Zhengzhou 451464, People's Republic of China

See page 4412 for the editorial comment on this article (doi: 10.1093/eurheartj/ehaa608)

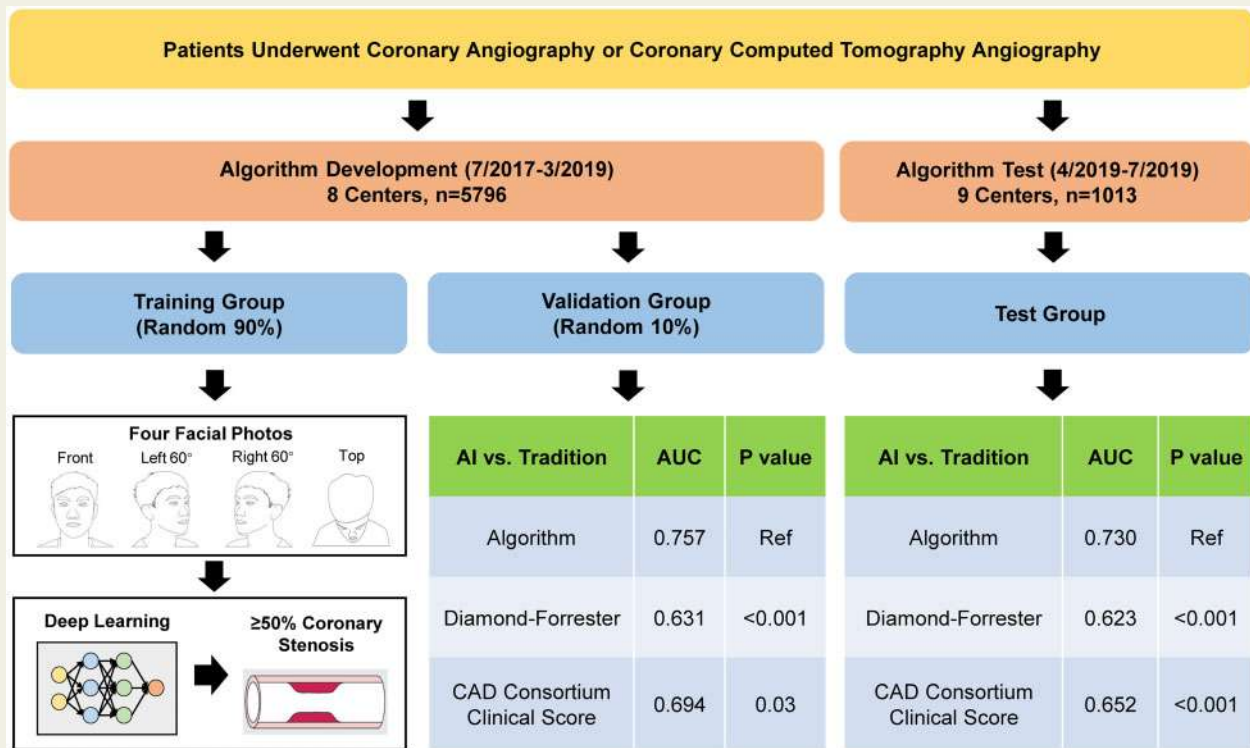|	
Aims	Facial features were associated with increased risk of coronary artery disease (CAD). We developed and validated a deep learning algorithm for detecting CAD based on facial photos.
Methods and results	We conducted a multicentre cross-sectional study of patients undergoing coronary angiography or computed tomography angiography at nine Chinese sites to train and validate a deep convolutional neural network for the detection of CAD (at least one ≥50% stenosis) from patient facial photos. Between July 2017 and March 2019, 5796 patients from eight sites were consecutively enrolled and randomly divided into training (90%, *n* = 5216) and validation (10%, *n* = 580) groups for algorithm development. Between April 2019 and July 2019, 1013 patients from nine sites were enrolled in test group for algorithm test. Sensitivity, specificity, and area under the receiver operating characteristic curve (AUC) were calculated using radiologist diagnosis as the reference standard. Using an operating cut point with high sensitivity, the CAD detection algorithm had sensitivity of 0.80 and specificity of 0.54 in the test group; the AUC was 0.730 (95% confidence interval, 0.699–0.761). The AUC for the algorithm was higher than that for the Diamond–Forrester model (0.730 vs. 0.623, *P* < 0.001) and the CAD consortium clinical score (0.730 vs. 0.652, *P* < 0.001).
Conclusion	Our results suggested that a deep learning algorithm based on facial photos can assist in CAD detection in this Chinese cohort. This technique may hold promise for pre-test CAD probability assessment in outpatient clinics or CAD screening in community. Further studies to develop a clinical available tool are warranted.

* Corresponding authors. Tel: +86-8839-6051, Fax: +86-8839-6051, Email: zhengzhe@fuwai.com (Z.Z.); Tel: +86- 6279-2481, Fax: +86-6279-2481, Email: xyji@tsinghua.edu.cn (X.J.)
† These authors contributed equally to this work.

Graphical Abstract

Patients Underwent Coronary Angiography or Coronary Computed Tomography Angiography		

Algorithm Development (7/2017-3/2019)
8 Centers, n=5796

Algorithm Test (4/2019-7/2019)
9 Centers, n=1013

Training Group (Random 90%)

Validation Group (Random 10%)

Test Group

Four Facial Photos
Front — Left 60° — Right 60° — Top

Deep Learning → ≥50% Coronary Stenosis

AI vs. Tradition	AUC	P value
Algorithm	0.757	Ref
Diamond-Forrester	0.631	<0.001
CAD Consortium Clinical Score	0.694	0.03

AI vs. Tradition	AUC	P value
Algorithm	0.730	Ref
Diamond-Forrester	0.623	<0.001
CAD Consortium Clinical Score	0.652	<0.001

Keywords   Deep learning • Coronary artery disease • Human face

Introduction

Coronary artery disease (CAD) remains the leading cause of death and chronic disability in cardiovascular diseases for all regions of the world.[1] Precise, practical and cost-effective tools to screen CAD are urgently needed. Except for conventional prediction models based on clinical risk factors,[2–9] some facial features were associated with increased risk of CAD, which might provide a potential means for disease screening.[10] For instance, alopecia, grey hair, facial wrinkle, earlobe crease, xanthelasmata, and arcus corneae were found to be probably associated with increased risk of CAD and poor cardiovascular health.[11–13] Further studies demonstrated that these facial features may have a fair performance in identifying CAD or improve the performance of traditional prediction model.[10,14]

However, use of such facial features for CAD screening has been limited by the (i) few categories and low prevalence of facial features, (ii) lack of specific definitions and quantifiable severity grading, and (iii) poor reproducibility in human identification.[10,11,15] A tool to integrate all facial features associated with CAD for disease screening is therefore warranted. As artificial intelligence has evolved, the deep learning algorithm has become a promising tool for disease diagnosis and prediction based on facial photos, especially for genetic and endocrine diseases.[16,17]

Thus, we hypothesized that this novel approach may help to integrate facial features for detecting CAD. And this study aimed to develop and validate a deep learning algorithm to detect CAD using facial photos.

Methods

Study design

We conducted a multicentre cross-sectional study. Data were obtained from two studies at nine sites in China (ClinicalTrials.gov identifiers NCT03214783 and NCT03731936). This study was approved by the institutional review boards of all the nine participating centres.

Participants

Patients undergoing elective coronary angiography or coronary computed tomography angiography (cCTA) were eligible for study inclusion. Exclusion criteria included the following: (i) prior percutaneous coronary intervention (PCI); (ii) prior coronary artery bypass graft (CABG); (iii) other heart diseases (e.g. congenital heart disease, valvular heart disease, or macrovascular disease); (iv) no blood biochemistry tests during the last 3 months; (v) artificial facial alteration (e.g. cosmetic surgery or facial trauma); and (vi) unable to be photographed. All eligible patients provided informed consent for participating the study and having their

photos used in research prior to the coronary angiography or cCTA procedure.

Study setting

The study was conducted in two phases. In phase one, eligible patients from eight sites were enrolled and partitioned randomly into training (90%) and validation (10%) groups for algorithm development. In phase two, eligible patients from nine sites were enrolled in a test group. Among these nine sites in phase two, eight also participated in phase one.

Data collection

Trained research nurses interviewed and photographed patients before the procedures. The baseline interviews collected data on socioeconomic status, lifestyle (alcohol, meat, fast food intake, and sports), clinical presentation, and family history and medications. Frontal, 60° profile, and head top views of each patient were photographed according to a standardized protocol using a digital camera (more than 20 million pixels) (Supplementary material online, *Method S1*). Medical records were abstracted after the procedure to obtain information on demographic characteristics, medical history, risk factors, and laboratory tests.

Labelling and facial photo pre-processing

All enrolled patients were dichotomized according to the presence of CAD, which was defined as at least one coronary lesion stenosis ≥50% based on coronary angiography or cCTA.[3,5–8] Two radiologists who were blinded to the study design independently reviewed each patient's angiogram or cCTA to assess the degree of coronary artery stenosis, with any disputes settled via review by a third radiologist for consensus decision. Coronary artery disease was further graded as one vessel, two vessels, three vessels, or left main disease according to the number and location of coronary vessels with ≥50% stenosis.

Facial photo quality was assessed by two investigators who were blinded to the study design according to the protocol in Supplementary material online, *Method S2*. Unqualified facial photos were excluded from final analysis. Qualified facial photos underwent further pre-processing using software to ensure uniformity of photo quality (Supplementary material online, *Method S2*).

Development of the models

Deep convolutional neural networks were used to train an algorithm for CAD detection (Supplementary material online, *Method S3, Figure S1*). We stacked four facial photos of each patient to a 12-channel photo to integrate all facial features. Given an integrated photo of the training set, the model extracted the useful features and performed the CAD classification decision. The prediction error was calculated by comparing the output with the ground truth according to the radiologist classification, and the parameters were adjusted accordingly to decrease the error. This process was repeated enough times to enable the network to learn to how to accurately assess significant CAD from facial photos. The parameters of the algorithm were fixed according to the best performance on validation set.

We also established three other CAD detection models for performance comparison. First, we fit a logistic regression model based on 26 baseline variables identified in previous pre-test CAD prediction models,[3–8] including patient demographic information, socioeconomic status, lifestyle, medical history, risk factors, and laboratory tests (Supplementary material online, *Table S1*). Second, we developed two hybrid models based on both facial photos and clinical variables, including one model that blended our algorithm with the three variables in the Diamond–Forrester model and another model that fused our algorithm

and the 26 variables in the logistic regression model (Supplementary material online, *Method S3*).

Evaluating the models

To evaluate the algorithm performance, we calculated the sensitivity, specificity, area under the receiver operating characteristic curve (AUC), positive predictive value (PPV), negative predictive value (NPV), and diagnostic accuracy rate using the radiologist diagnosis as the comparator. We evaluated the algorithm at two operating points selected from the receiver operating characteristic (ROC) curve; one was selected for the maximum sum of sensitivity and specificity and the other for high (80%) sensitivity.

Understanding the algorithm

We conducted several analyses to better understand how CAD was identified over many layers in the deep learning algorithm.

CAD risk factor prediction

We hypothesized that the algorithm may, in part, detect CAD by identifying CAD risk factors. Thus, we trained other seven algorithms based on facial photos to, respectively, predict seven CAD risk factors that have been included in traditional models, including age, sex, diabetes, hypertension, hyperlipidaemia, smoking, and body mass index (BMI) (Supplementary material online, *Method S4.1*).[3–7,9] And we, respectively, test the seven algorithms performance in the test group to speculate the potential working mechanisms of the algorithm identifying CAD.

Visualization tests

Using data from the training group, we conducted two visualization tests to identify the facial regions highlighted as important for the classification of CAD by the algorithm (Supplementary material online, *Method S4.2*). In the first test, we used automatic landmark identification software to divide patients' frontal facial photo into the following seven parts: bilateral cheeks, forehead, bilateral eyes, bilateral ears, nose, mouth, and chin. We in turn occluded each one of these parts to retrain and validate the algorithm. We evaluated the contribution of the different facial areas to the algorithm based on the decrease in algorithm performance after the occlusion (Supplementary material online, *Figure S2A*).

In the second visualization test, we in turn occluded smaller areas (11×11 pixels) from all the facial photos. The impact of the occlusion on the algorithm was used to output a heatmap of each photo, which more intuitively showed the facial areas considered important for CAD classification by the algorithm (Supplementary material online, *Figure S2B*).

Dose–response relationship test

To further examine the robustness of the association between facial features and CAD, we assessed the dose–response relationship between the number of 'positive facial areas' and CAD prevalence in the training dataset (Supplementary material online, *Method S4.3*). To identify the positive facial areas, we used automatic landmark software to divide patients' frontal facial photo into nine parts, including left cheek, right cheek, forehead, left eye, right eye, bilateral ears, nose, mouth, and chin (Supplementary material online, *Figure S2A*). Positive areas were those that contributed to the detection of CAD, and they were identified by a decrease in the AUC of the model after occluding those specific areas of the photos. We divided patients into three groups based on the number of positive facial areas (0–3, 4–6, or 6–9 positive facial areas) and compared the prevalence of CAD, one-/two-vessel disease, and three-vessel/left main disease among these groups.
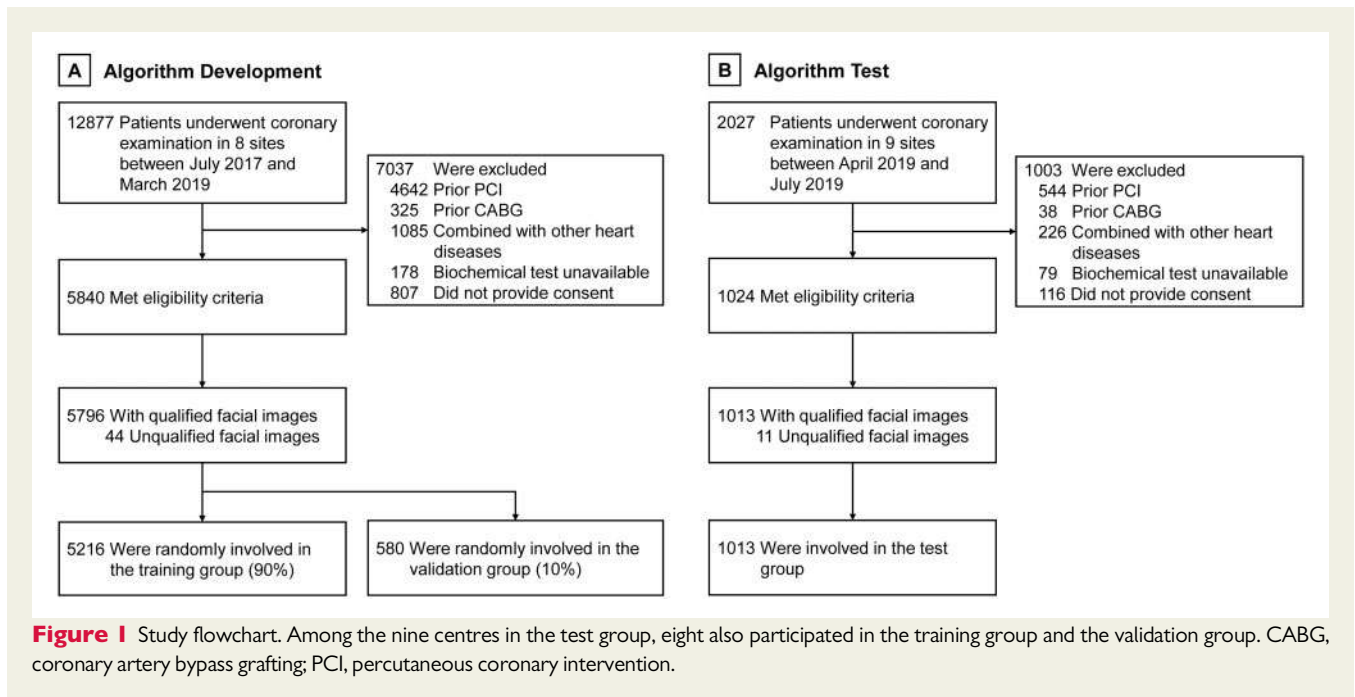
Figure 1 Study flowchart. Among the nine centres in the test group, eight also participated in the training group and the validation group. CABG, coronary artery bypass grafting; PCI, percutaneous coronary intervention.

Statistical analysis

Based on the results of validation group, we hypothesized that our algorithm would have a sensitivity of 0.8 and specificity of 0.6 in the test group. The sampling precision of the sensitivity calculation was estimated at ±5% with a 5% significance level. Thus, we needed to enrol 246 patients with CAD and 369 patients without CAD in the test group to detect the sensitivity and specificity of the algorithm.[18]

Data are presented as mean ± standard deviation for continuous variables and percentages for discrete variables. Categorical variables were compared using chi-square or Fisher's exact tests, and continuous variables were compared using t or Mann–Whitney U tests.

Exact 95% confidence intervals (CIs) were calculated for all measures of diagnostic performance. We used Delong tests to compare the AUC of different models. Pre-specified subgroup analyses were conducted according to age, sex, angina symptom, risk factors, and extent of coronary lesions. To further robust our results, we performed two sensitivity analyses, including (i) using photos with increased or decreased pixels to assess the algorithm performance in different image quality and (ii) testing the algorithm performance in the extra centre that was not included in the development phase.

All comparisons were two-sided, with statistical significance defined as $P < 0.05$. Analyses were calculated using SAS version 9.4 (SAS Institute Inc.).

Results

Study population

Between July 2017 and March 2019, 5840 patients who met the criteria for inclusion were enrolled across eight sites (*Figure 1*). We excluded 44 patients (0.8%) with unqualified facial photos. Among the remaining 5796 patients, we randomly divided 90% ($n = 5216$) into the training group and 10% ($n = 580$) into the validation group. The baseline characteristics were similar in the two groups (*Table 1*).

Between April 2019 and July 2019, 1024 eligible patients were enrolled at nine sites for inclusion in the test group; the final dataset included 1013 patients after excluding 11 (1.1%) patients with unqualified facial photos (*Figure 1*). Compared with patients in the training group, those in the test group were older, more likely to have undergone cCTA, and less likely to be male, have cardiac risk factors, have lifestyle risk factors, and be undergoing medical therapy (*Table 1*).

Model performance in validation dataset

The AUC, sensitivity, specificity, PPV, NPV, and accuracy of the algorithm and other models are presented in *Table 2*, Supplementary material online, *Table S2*, and *Figure 2*. The algorithm achieved an AUC of 0.757 (95% CI, 0.710–0.805) in the validation group and 0.730 (95% CI, 0.699–0.761) in the test group. Using the operating point with the maximum sum of sensitivity and specificity, the algorithm had sensitivity of 0.71 and specificity of 0.72 in the validation and sensitivity of 0.68 and specificity of 0.68 in the test group. These results corresponded to a PPV of 0.89 and NPV of 0.42 in the validation group and PPV of 0.72 and NPV of 0.64 in the test group. Using the operating point with high sensitivity (80%), the algorithm had sensitivities and specificities, respectively, of 0.80 and 0.61 for the validation group and 0.80 and 0.54 in the test group. In the test dataset, the algorithm exhibited a higher AUC when compared with the Diamond–Forrester model (0.730 vs. 0.623, $P < 0.001$), the CAD consortium clinical score (0.730 vs. 0.652, $P < 0.001$) and the logistic regression model based on 26 baseline variables (0.730 vs. 0.660, $P < 0.001$). The addition of the three variables in the Diamond–Forrester (0.730 vs. 0.726, $P = 0.66$) and the 26 variables in the logistic regression models (0.730 vs. 0.724, $P = 0.52$) did not significantly improve the AUC of the algorithm.

Figure 3 summarizes the algorithm performance in subgroups of the test dataset. The algorithm had similar performance in male and

Table 1 Baseline characteristics

Characteristics	Training group, N = 5216	Validation group, N = 580	P-value[a]	Test group, N = 1013	P-value[b]
Age, years	59.2 ± 9.2	59.4 ± 9.2	0.66	61.3 ± 10.3	<0.001
Male	3810 (73.0)	401 (69.1)	0.05	579 (57.1)	<0.001
Han ethnicity	4977 (95.4)	543 (93.6)	0.05	1001 (98.7)	<0.001
Birthplace			0.20		<0.001
East	1077 (20.6)	115 (19.8)		471 (46.5)	
Northeast	617 (11.8)	61 (10.5)		66 (6.5)	
North	2971 (57.0)	328 (56.6)		351 (34.6)	
Northwest	118 (2.3)	16 (2.8)		13 (1.3)	
South Central	371 (7.1)	56 (9.7)		105 (10.4)	
Southwest	62 (1.2)	4 (0.7)		7 (0.7)	
Education			0.89		0.001
Less than high school	2462 (47.2)	277 (47.8)		524 (51.7)	
High school	1405 (26.9)	158 (27.2)		288 (28.4)	
University	1291 (24.8)	137 (23.6)		194 (19.1)	
Postgraduate or above	58 (1.1)	8 (1.4)		8 (0.8)	
Sedentary work	1221 (23.4)	124 (21.4)	0.27	173 (17.1)	<0.001
Work time			0.09		<0.001
<8 h/day	663 (12.7)	83 (14.3)		127 (12.5)	
8–10 h/day	1209 (23.2)	127 (21.9)		164 (16.2)	
>10 h/day	252 (4.8)	16 (2.8)		34 (3.4)	
Unemployed or retired	3092 (59.3)	354 (61.0)		689 (67.9)	
Lifestyle					
Alcohol (>2 times/week for >1 year)	1373 (26.3)	141 (24.3)	0.30	188 (18.5)	<0.001
Meat (>2 times/week, >300 g/time)	1216 (23.3)	143 (24.7)	0.47	103 (10.2)	<0.001
Fast food (>4 times/week)	387 (7.4)	36 (6.2)	0.29	24 (2.4)	<0.001
Sport (aerobic exercise >1 hour)			0.39		<0.001
≥3 times/week	2708 (51.9)	293 (50.5)		376 (37.1)	
1–2 times/week	911 (17.5)	94 (16.2)		105 (10.4)	
Never	1597 (30.6)	193 (33.3)		533 (52.6)	
Smoking (pack years)	2.5 (0–29.3)	0 (0–28.0)	0.06	0 (0–15)	<0.001
BMI	25.7 ± 3.2	25.8 ± 3.3	0.32	25.3 ± 3.4	0.001
Family history	883 (16.9)	85 (14.7)	0.16	258 (25.4)	0.001
Hypertension	3228 (61.9)	357 (61.6)	0.88	551 (54.3)	<0.001
Hyperlipidaemia	3970 (76.1)	428 (73.8)	0.22	358 (35.3)	<0.001
Diabetes	1457 (27.9)	177 (30.5)	0.19	235 (23.2)	0.002
Cerebrovascular disease	582 (11.2)	58 (10.0)	0.40	62 (6.1)	<0.001
Heart failure	86 (1.6)	13 (2.2)	0.30	21 (2.1)	0.34
Peripheral vascular disease	329 (6.3)	41 (7.1)	0.48	57 (5.6)	0.41
Chronic renal disease	48 (0.9)	8 (1.4)	0.28	26 (2.6)	<0.001
COPD	68 (1.3)	7 (1.2)	0.85	27 (2.7)	0.001
Symptom			0.86		<0.001
No symptom	603 (11.6)	72 (12.4)		98 (9.7)	
Non-angina	965 (18.5)	102 (17.6)		285 (28.1)	
Atypical angina	1952 (37.4)	222 (38.3)		406 (40.0)	
Typical angina	1696 (32.5)	184 (31.7)		225 (22.2)	
Medication					
Aspirin	2927 (56.1)	325 (56.0)	0.97	416 (41.0)	<0.001
Clopidogrel	1154 (22.1)	129 (22.2)	0.95	159 (15.7)	<0.001
β-blocker	1439 (27.6)	162 (27.9)	0.86	225 (22.2)	<0.001
Statins	2387 (45.8)	260 (44.8)	0.67	402 (39.6)	<0.001
ACEI	483 (9.3)	67 (11.6)	0.07	87 (8.6)	0.50

Continued

Table I *Continued*

Characteristics	Training group, N = 5216	Validation group, N = 580	P-value[a]	Test group, N = 1013	P-value[b]
CCB	1280 (24.5)	137 (23.6)	0.63	211 (20.8)	0.01
Long-acting nitrate	1134 (21.7)	128 (22.1)	0.86	134 (13.2)	<0.001
Serum glucose, mmol/L	5.99 ± 1.97	5.99 ± 1.95	0.42	5.94 ± 1.92	0.03
Total cholesterol, mmol/L	4.16 ± 1.11	4.19 ± 1.13	0.58	4.52 ± 1.15	0.01
Triglycerides, mmol/L	1.64 ± 1.14	1.65 ± 1.03	0.94	1.68 ± 1.12	0.26
HDL, mmol/L	1.19 ± 0.32	1.18 ± 0.32	0.85	1.23 ± 0.34	0.006
LDL, mmol/L	2.45 ± 0.90	2.46 ± 0.91	0.98	2.58 ± 0.87	0.76
Lesion severity			0.87		<0.001
No coronary stenosis	1178 (22.6)	134 (23.1)		467 (46.1)	
One vessel	1041 (20.0)	118 (20.3)		220 (21.7)	
Two vessels	1037 (19.9)	107 (18.4)		144 (14.2)	
Three vessels	1490 (28.6)	173 (29.8)		149 (14.7)	
Left main	470 (9.0)	48 (8.3)		34 (3.4)	
Coronary test			0.93		<0.001
Coronary angiography	4638 (88.9)	515 (88.8)		745 (73.5)	
Computed tomography	578 (11.1)	65 (11.2)		269 (26.5)	

Data presented as mean ± standard deviation or n (%). No data were missing in *Table 1*.
ACEI, angiotensin-converting enzyme inhibitor; BMI, body mass index; CCB, calcium channel blocker; COPD, chronic obstructive pulmonary disease; HDL, high-density lipoprotein; LDL, low-density lipoprotein.
[a]P-value was obtained by comparison of the training and validation groups.
[b]P-value was obtained by comparison of the training and test groups.

female patients and had better performance in patients with typical angina, more CAD risk factors, <60 years old or more complex lesions. In sensitivity analysis of changing photo pixels, the algorithm performance remained stable (Supplementary material online, *Figure S3*). In another sensitivity analysis of performance test in the extra centre (n = 16) that was not included in the development phase, the AUC was 0.436.

Algorithm performance in predicting CAD risk factors

For the continuous risk factors, the algorithm achieved a mean absolute error (MAE) of 5.68 (95% CI, 5.41–5.95) for age and 2.59 (95% CI, 2.45–2.72) for BMI (*Table 3*). For categorical risk factors, the algorithm achieved an AUC of 0.990 for sex, 0.694 for hyperlipidaemia, 0.579 for diabetes, 0.606 for hypertension, and 0.831 for smoking (*Table 3*).

Visualization results

After occluding each of the seven facial parts, the largest decrease in AUC was found for the cheek (△AUC = 0.0365), followed by the forehead (△AUC = 0.0185), nose (△AUC = 0.0178), eyes (△AUC = 0.0160), mouth (△AUC = 0.0154), ears (△AUC = 0.0148), and chin (△AUC = 0.0062) (*Figure 4A*). In tests occluding regions of 11 × 11 pixels, we randomly selected 10% of patients (n = 522) from the training group and successfully obtained 2088 heatmaps identifying the regions that the algorithm might have used to make its prediction. *Figure 4B* shows the specific facial features highlighted by the algorithm.

Dose–response relationship between facial areas and CAD

There was a trend of higher prevalence of CAD (P < 0.001), one-/two-vessel disease (P < 0.001), and three-vessel/left main disease (P < 0.001) as the number of positive facial areas increased (*Figure 4C*).

Discussion

In this large multicentre cross-sectional study, we found that a deep learning algorithm based on facial photos had a moderate performance in detecting CAD (*Take home figure*). The algorithm had an AUC of 0.730 (95% CI 0.699–0.761), sensitivity of 0.80, and specificity of 0.54 in the test group. Furthermore, the algorithm had a higher AUC when compared with the Diamond–Forrester model (0.730 vs. 0.623, P < 0.001) and the CAD consortium clinical score (0.730 vs. 0.652, P < 0.001).

Our study further clarified the feasibility of using human facial features to detecting CAD. Christoffersen et al.[10] previously found that male pattern baldness, earlobe crease, and xanthelasmata further improve risk classification of the Framingham risk model, especially for individuals of intermediate risk. In another cross-sectional study (n = 558), Wang et al.[14] demonstrated that diagonal earlobe creases had a sensitivity of 78% and specificity of 61% for identifying CAD (one or more ≥50% stenosis). However, prior studies have been unable to integrate all CAD-related facial features to predict CAD, relied on subjective inspection of facial features, and lacked validation of a separate dataset. In the present study, we developed and

Table 2   Performance of different models for detecting coronary artery disease

Models	AUC (95% CI)	Sensitivity	Specificity	PPV	NPV	Accuracy	*P*-value
Validation dataset (Max Sen+Spe)[a]							
Algorithm	0.757 (0.710–0.805)	0.71	0.72	0.89	0.43	0.71	Ref
Diamond–Forrester model	0.631 (0.579–0.683)	0.27	0.93	0.92	0.28	0.42	<0.001
CAD consortium clinical score	0.694 (0.645–0.743)	0.57	0.72	0.87	0.34	0.60	0.03
Logistic Regression Model[b]	0.750 (0.701–0.799)	0.78	0.62	0.87	0.46	0.74	0.79
Algorithm + Diamond–Forrester model	0.755 (0.710–0.805)	0.63	0.78	0.90	0.39	0.67	0.87
Algorithm + logistic regression model	0.786 (0.740–0.833)	0.76	0.72	0.90	0.47	0.75	0.08
Validation dataset (Sen = 0.8)[a]							
Algorithm	0.757 (0.710–0.805)	0.80	0.61	0.87	0.47	0.75	Ref
Diamond–Forrester model	0.631 (0.579–0.683)	0.82	0.31	0.80	0.34	0.70	<0.001
CAD consortium clinical score	0.694 (0.645–0.743)	0.81	0.39	0.82	0.39	0.72	0.03
Logistic regression model[b]	0.750 (0.701–0.799)	0.80	0.59	0.87	0.47	0.75	0.79
Algorithm + Diamond–Forrester Model	0.755 (0.710–0.805)	0.80	0.57	0.86	0.46	0.75	0.87
Algorithm + logistic regression model	0.786 (0.740–0.833)	0.80	0.65	0.88	0.49	0.76	0.08
Test dataset (Max Sen+Spe)[c]							
Algorithm	0.730 (0.699–0.761)	0.68	0.68	0.72	0.64	0.68	Ref
Diamond–Forrester model	0.623 (0.588–0.657)	0.49	0.69	0.65	0.54	0.58	<0.001
CAD consortium clinical score	0.652 (0.618–0.686)	0.73	0.50	0.63	0.61	0.63	<0.001
Logistic regression model[b]	0.660 (0.626–0.693)	0.60	0.66	0.67	0.58	0.63	<0.001
Algorithm + Diamond–Forrester Model	0.726 (0.695–0.757)	0.76	0.60	0.69	0.68	0.69	0.66
Algorithm + logistic regression model	0.724 (0.693–0.755)	0.71	0.63	0.69	0.65	0.67	0.52
Test dataset (Sen = 0.8)[c]							
Algorithm	0.730 (0.699–0.761)	0.80	0.54	0.66	0.68	0.67	Ref
Diamond–Forrester model	0.623 (0.588–0.657)	0.82	0.31	0.58	0.59	0.58	<0.001
CAD consortium clinical score	0.652 (0.618–0.686)	0.81	0.61	0.61	0.63	0.61	0.001
Logistic regression model[b]	0.660 (0.626–0.693)	0.80	0.40	0.61	0.62	0.61	<0.001
Algorithm + Diamond–Forrester model	0.726 (0.695–0.757)	0.80	0.53	0.67	0.69	0.67	0.66
Algorithm + logistic regression model	0.724 (0.693–0.755)	0.80	0.49	0.65	0.67	0.65	0.52

AUC, area under the receiver operating characteristic curve; NPV, negative predictive value; PPV, positive predictive value; Sen, sensitivity; Spe, specificity.
[a]Prevalence of CAD (one coronary lesion ≥50%) in the validation group was 76.9% (446/580).
[b]The logistic regression model included the following baseline variables: age, sex, education, sedentary work, work time, lifestyle, sport, smoking, body mass index, family history of coronary artery disease, hypertension, hyperlipidaemia, diabetes, cerebrovascular disease, heart failure, peripheral vascular disease, chronic renal disease, chronic obstructive pulmonary disease, symptoms, serum glucose, total cholesterol, triglycerides, high-density lipoprotein cholesterol, and low-density lipoprotein cholesterol. This model included all variables in traditional and updated coronary artery disease prediction models.[3–8]
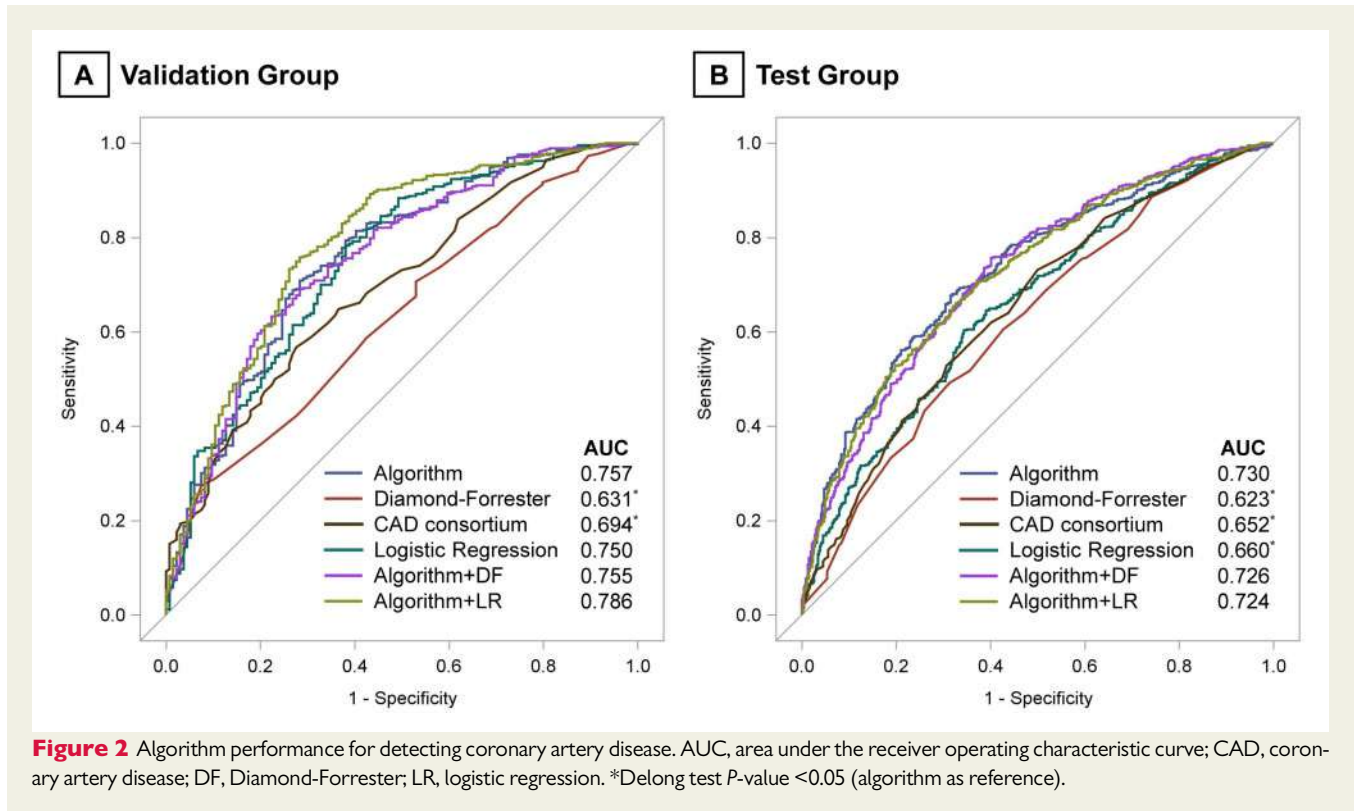[c]Prevalence of CAD (one coronary lesion ≥50%) in the test group was 53.9% (546/1013).

validated a deep learning algorithm that integrated patients' facial information from photos to detect CAD. The algorithm had moderate performance (AUC 0.730, sensitivity 0.80, specificity 0.54) in our test dataset, and it outperformed the traditional Diamond–Forrester model and the widely used CAD consortium model.[5,9] Furthermore, the addition of clinical variables did not improve the algorithm performance, which meant that the algorithm could be easily used based on only facial photos without additional medical history or examination. Our study demonstrated the feasibility of a deep learning algorithm based on human facial photos for CAD screening.

Our findings are plausible according to several analyses to understand the algorithm. First, our hypothesis that the algorithm may, in part, predict CAD by identifying CAD risk factors can be speculated by our results showing analysing facial photo also precisely predicted cardiovascular risk factors. AUC of 0.99 for sex conformed to the common sense that sex may be easily determined by facial photos. AUC of other risk factors ranged from 0.58 to 0.83, which were

consistent with prior small-sample studies.[19–21] Further supporting our hypothesis, the addition of clinical variables to the algorithm resulted in no significant improvement in performance. Second, our occlusion tests confirmed that many facial regions highlighted by the algorithm were consistent with those identified in prior studies, such as male pattern baldness, frontoparietal baldness, and earlobe crease.[10,11] Third, we confirmed a dose–response relationship between the number of facial regions considered important for CAD classification by the algorithm and CAD prevalence. Collectively, these results highlight the reliability and scientific basis of the algorithm.

Interestingly, in visualization tests, the cheek, forehead, and nose contributed more to our algorithm than other facial areas. These results differ from those of previous reports showing features of the eyes, ears, and hair were more likely to be associated with CAD.[10,11] There are several potential explanations for these findings. First, the photo pre-processing used in our study may have influenced the

Figure 2 Algorithm performance for detecting coronary artery disease. AUC, area under the receiver operating characteristic curve; CAD, coronary artery disease; DF, Diamond-Forrester; LR, logistic regression. *Delong test *P*-value <0.05 (algorithm as reference).

classification outcomes. In visualization tests, we reduced the photo resolution to 256×256 pixels and used only frontal photos for the deep learning algorithm. Features of the eyes, ears, and hair may not have been clear enough under these circumstances for accurate classification decisions. Second, our deep learning algorithm may have extracted some features that are strongly associated with CAD but are beyond human perception or understanding. For example, perceived age, facial adiposity, and shapes have been associated with human cardiovascular health, but it has been difficult to quantify these features and conduct studies to confirm the conclusions.[19,20,22] A deep learning algorithm is well-suited for such applications. For instance, Zhao et al.[23] successfully used facial recognition techniques to quantitatively analyse the results of facial inspection for health status prediction, which is an important but complex diagnostic tool in traditional Chinese medicine. Our algorithm may integrate such abstract features for CAD prediction. Third, the association between CAD and features of the cheek, forehead, and nose may have been misestimated in previous studies because of the reliance on investigators' subjective assessments of wrinkles and deep pouches, among other features. Results from our occlusion tests suggest that further evaluation of the association between these facial features and cardiac health as well as the associated mechanisms may be warranted.

There are two potential application scenarios for our algorithm. First, as a convenient algorithm which performed better than Diamond–Forrester model, our algorithm can assist to assess the pre-test CAD probability to help guide further diagnostic tests. Several notable models have been develop to assess pre-test CAD probability.[3–8] The Diamond–Forrester model was a landmark work published in 1979 to determine the pre-test CAD probability based on age, sex, and type of chest pain.[3] This model was simple enough for routine clinical use.[5] However, the obsolescence of model development population made it overestimates CAD risk in more contemporary populations.[24] Updated models including additional risk factors have improved performance and generalizability, but the multidimensional variables increased the difficulty in clinical application.[13–17] Compared with traditional models, our algorithm had a better performance, which may support our algorithm to assist in pre-test CAD probability assessment or even to be an adjunctive test for further diagnostic test, such as exercise treadmills etc., particularly in patients with <60 years old, typical angina or more CAD risk factors. Second, the algorithm may hold promise for early CAD screener in high-risk community populations. The algorithm could be developed as a self-reported mobile application for use in high-risk community populations to assess CAD risk in advance of a medical visit, with the results used to support a patient-centred discussion on cardiovascular health. Further algorithm refinement and validation based on community populations are warranted.

Study limitations
This study has several limitations. First, we only examined Chinese patients, and our findings may not generalize to populations of other ethnicities. But this may not influence our study to achieve our primary aim of assessing the feasibility of detecting CAD based on facial photos using deep learning. Future cohorts can use transfer learning
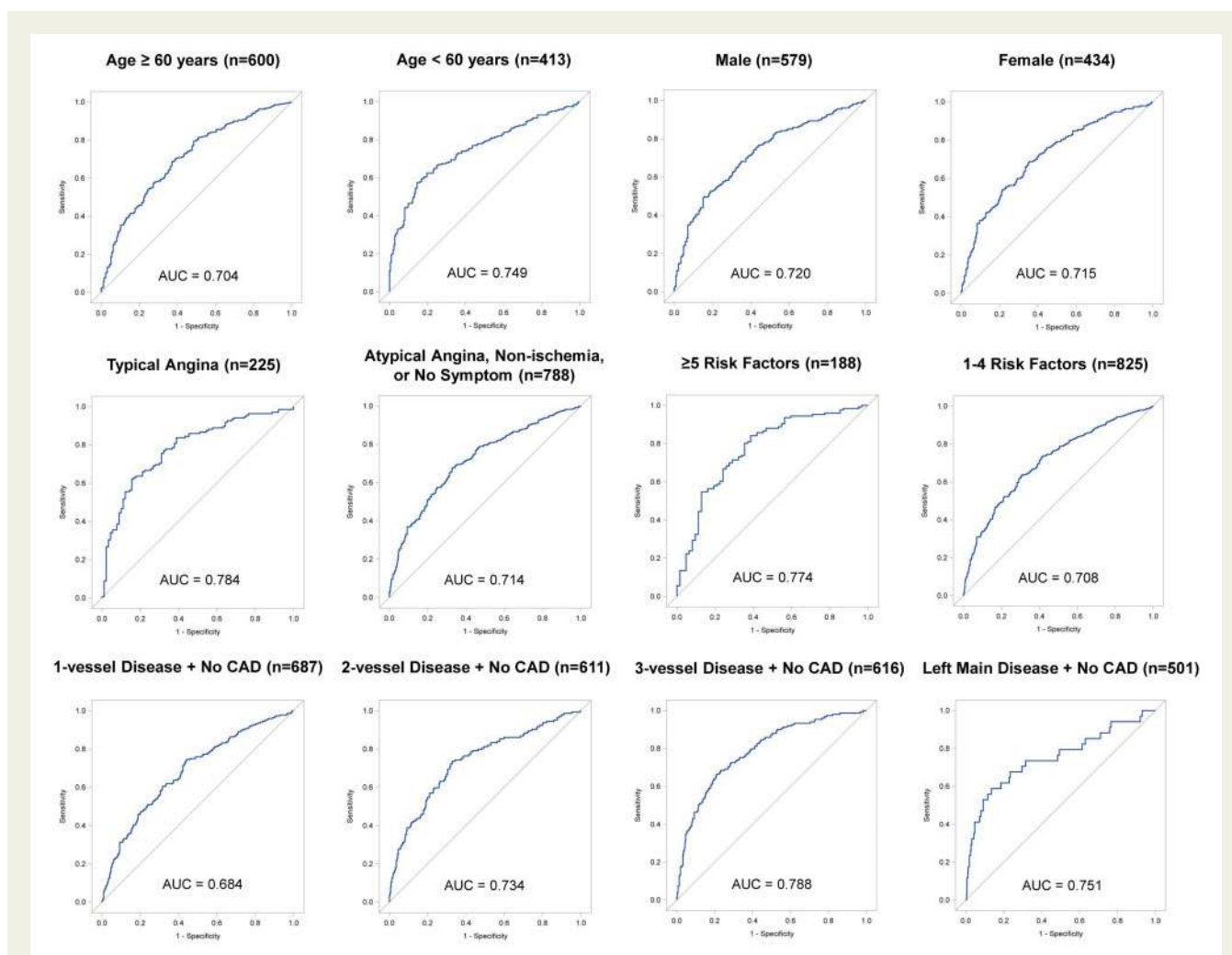
Figure 3 Algorithm performance in subgroups of test group. AUC, area under the receiver operating characteristic curve; CAD, coronary artery disease. Subgroup analyses of coronary artery disease risk factors were grouped based on the presence of ≥5 of the following risk factors: age >60 years, male sex, diabetes mellitus, hypertension, hyperlipidaemia, body mass index ≥25 kg/m^2, and current or ex-smoker.

from ResNet-50 or our algorithm to replicate or to further expand towards other descent. Second, significant CAD was defined based on coronary angiography or cCTA—the selection between these two modalities may bias the outcomes. But we believed that the bias was small, as 64-row cCTA was found to have reasonably consistent diagnostic performance when compared with coronary angiography.[25] In the present study, the concordance rate of cCTA and subsequent coronary angiography performed within 3 months was 93.1% in detecting coronary stenosis ≥50% (Supplementary material online, *Table S3*). Third, angiography was reviewed by well-trained radiologists, rather than interventional, general cardiologists or quantitative coronary angiography, which even though was very unlikely to bias the outcomes. Fourth, only one centre in the test group was different from those in the model development group, potentially limiting the generalizability of the algorithm. In this centre, both the small-sample size and patient heterogeneity could lead to this lower AUC (0.436). Thus, further external validation is still warranted. Thus, further external validation is still warranted. Even so,

Table 3 Predicting risk factors of coronary artery disease by algorithm

Risk factors	AUC (95% CI)	MAE (95% CI)
Continuous variables		
Age	–	5.68 (5.41–5.95)
Body mass index	—	2.59 (2.45–2.72)
Categorical variables		
Male sex	0.990 (0.982–0.997)	—
Hyperlipidaemia	0.694 (0.658–0.730)	—
Diabetes mellitus	0.579 (0.538–0.621)	—
Hypertension	0.606 (0.571–0.641)	—
Current or ex-smoker	0.831 (0.805–0.856)	—

The algorithm performance in predicting coronary artery disease risk factors was assessed in the test group.
AUC, area under the receiver operating characteristic curve; CI, confidence interval; MAE, mean absolute error.
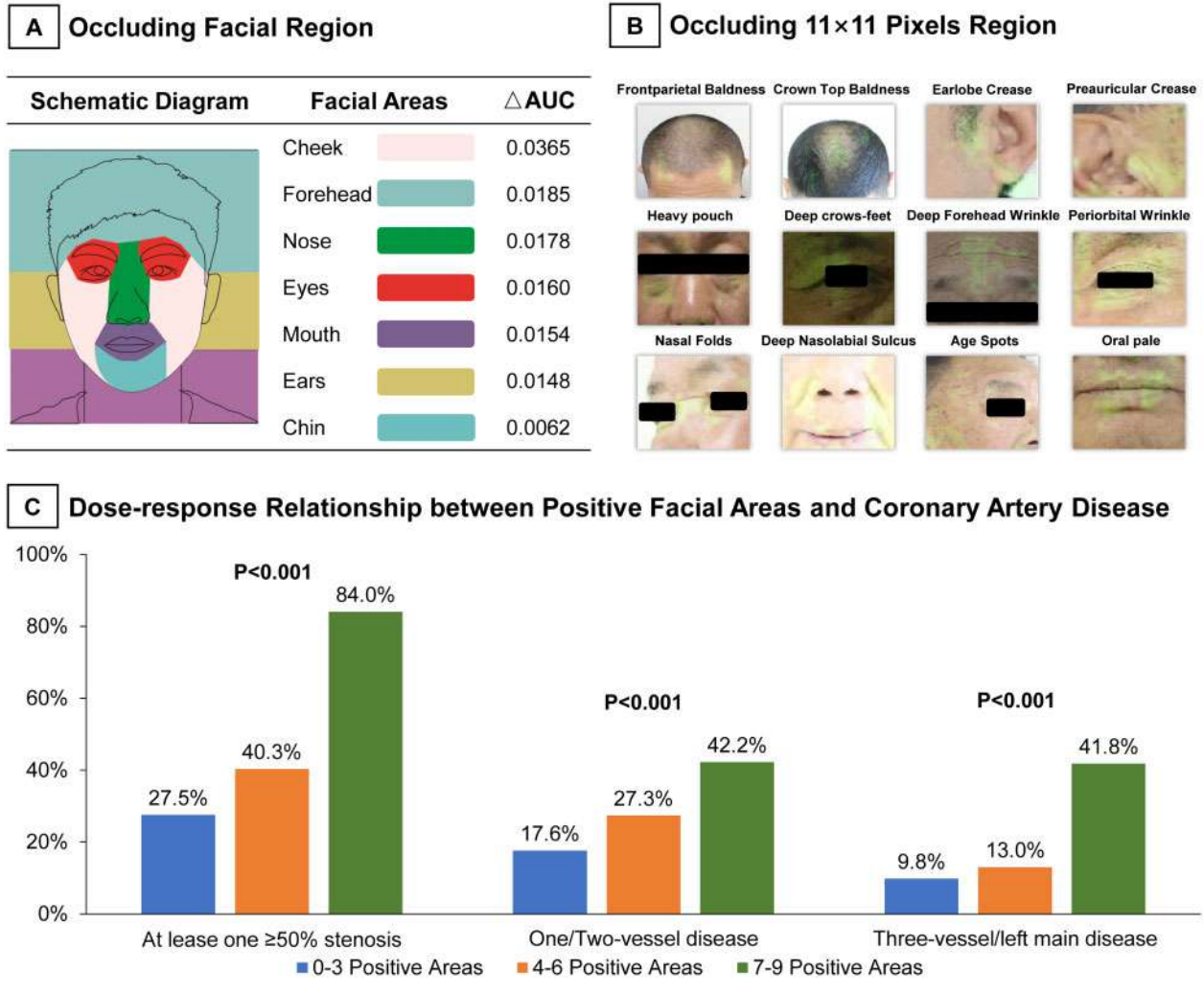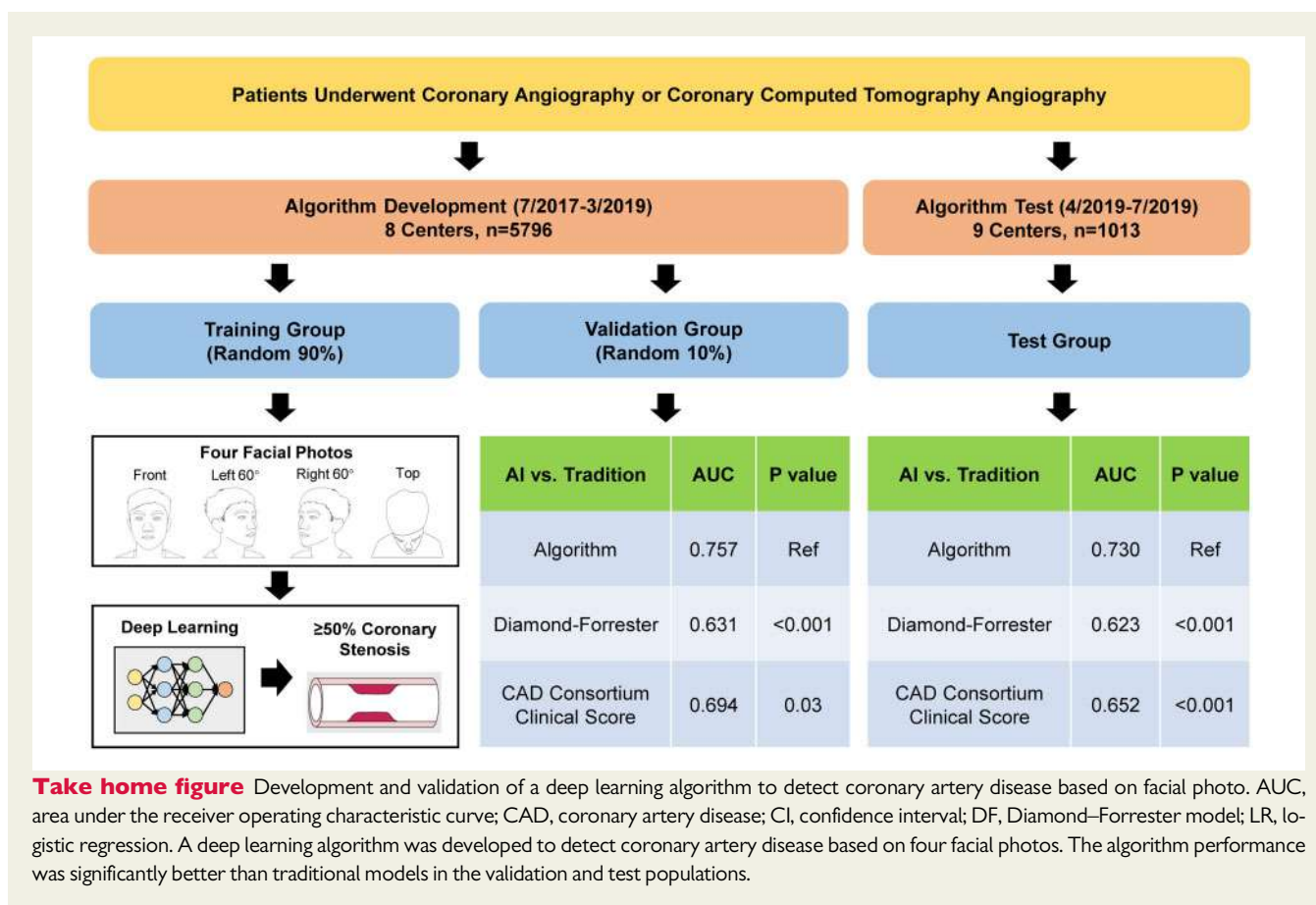
Figure 4 Results of occlusion and dose–response relationship tests. AUC, area under the receiver operating characteristic curve. In tests occluding facial regions (A), △AUC was defined as the decrease in algorithm performance after occluding a specific facial region. In tests occluding regions of 11 × 11 pixels (B), the green regions were highlighted by the algorithm as important for detecting CAD. In the dose–response relationship test (C), the positive facial areas were judged based on the change in algorithm performance after occlusion.

the large population heterogeneity between training and test periods, which was attributed to the different time of starting enrolment in each hospital, suggested the robust performance of our facial algorithm. Fifth, for CAD screening, the low specificity and upwards of 46% false-positive results may cause anxiety and inconvenience for patients. Thus, target populations who have a relatively high CAD risk and could benefit most from the algorithm should be explored. Finally, our study aim was only to evaluate the feasibility of using deep learning algorithm to detect CAD based on facial photos. Thus, the algorithm in its current form is not optimized for use in clinical practice. The algorithm requires further development and validation based on the target outpatient or community populations. In addition, methods to reduce the photo quality requirements and simplify the photography processes should be explored to make

the algorithm better meet the needs of real-world application. Furthermore, privacy protection, availability of this technology on insurance, and other social implications should be concerned in further work.

Conclusions

Our results proposed a new concept where facial analysis using deep learning can help to detect CAD in this large study of Chinese population. This effort supported a potential step towards the development of a deep learning-based tool for the pre-test CAD probabilities assessment in outpatient clinics or the CAD screening in community, which may help to guide further diagnostic testing or medical visit.

Take home figure Development and validation of a deep learning algorithm to detect coronary artery disease based on facial photo. AUC, area under the receiver operating characteristic curve; CAD, coronary artery disease; CI, confidence interval; DF, Diamond–Forrester model; LR, logistic regression. A deep learning algorithm was developed to detect coronary artery disease based on four facial photos. The algorithm performance was significantly better than traditional models in the validation and test populations.

Supplementary material

Supplementary material is available at *European Heart Journal* online.

Declaration of Helsinki

The authors state that their study complies with the Declaration of Helsinki that the institutional ethics committees of all the participating centres have approved the research protocol and that informed consent has been obtained from all the patients.

References

1. Roth GA, Johnson C, Abajobir A, Abd-Allah F, Abera SF, Abyu G, Ahmed M, Aksut B, Alam T, Alam K, Alla F, Alvis-Guzman N, Amrock S, Ansari H, Arnlov J, Asayesh H, Atey TM, Avila-Burgos L, Awasthi A, Banerjee A, Barac A, Barnighausen T, Barregard L, Bedi N, Belay Ketema E, Bennett D, Berhe G, Bhutta Z, Bitew S, Carapetis J, Carrero JJ, Malta DC, Castaneda-Orjuela CA, Castillo-Rivas J, Catala-Lopez F, Choi JY, Christensen H, Cirillo M, Cooper L Jr, Criqui M, Cundiff D, Damasceno A, Dandona L, Dandona R, Davletov K, Dharmaratne S, Dorairaj P, Dubey M, Ehrenkranz R, El Sayed Zaki M, Faraon EJA, Esteghamati A, Farid T, Farvid M, Feigin V, Ding EL, Fowkes G, Gebrehiwot T, Gillum R, Gold A, Gona P, Gupta R, Habtewold TD, Hafezi-Nejad N, Hailu T, Hailu GB, Hankey G, Hassen HY, Abate KH, Havmoeller R, Hay SI, Horino M, Hotez PJ, Jacobsen K, James S, Javanbakht M, Jeemon P, John D, Jonas J, Kalkonde Y, Karimkhani C, Kasaeian A, Khader Y, Khan A, Khang YH, Khera S, Khoja AT, Khubchandani J, Kim D, Kolte D, Kosen S, Krohn KJ, Kumar GA, Kwan GF, Lal DK, Larsson A, Linn S, Lopez A, Lotufo PA, El Razek HMA, Malekzadeh R, Mazidi M, Meier T, Meles KG, Mensah G, Meretoja A, Mezgebe H, Miller T, Mirrakhimov E, Mohammed S, Moran AE, Musa KI, Narula J, Neal B, Ngalesoni F, Nguyen G, Obermeyer CM, Owolabi M, Patton G, Pedro J, Qato D, Qorbani M, Rahimi K, Rai RK, Rawaf S, Ribeiro A, Safiri S, Salomon JA, Santos I, Santric Milicevic M, Sartorius B, Schutte A, Sepanlou S, Shaikh MA, Shin MJ, Shishehbor M, Shore H, Silva DAS, Sobngwi E, Stranges S, Swaminathan S, Tabares-Seisdedos R, Tadele Atnafu N, Tesfay F, Thakur JS, Thrift A, Topor-Madry R, Truelsen T, Tyrovolas S, Ukwaja KN, Uthman O, Vasankari T, Vlassov V, Vollset SE, Wakayo T, Watkins D, Weintraub R, Werdecker A, Westerman R, Wiysonge CS, Wolfe C, Workicho A, Xu G, Yano Y, Yip P, Yonemoto N, Younis M, Yu C, Vos T, Naghavi M, Murray C. Regional, and national burden of cardiovascular diseases for 10 causes, 1990 to 2015. *J Am Coll Cardiol* 2017;**70**: 1–25.

2. Peter WF, Ralph BD, Daniel L, Belanger AM, Silbershatz H, Kannel WB. Prediction of coronary heart disease using risk factor categories. *Circulation* 1998; **97**:1837–1847.

3. Diamond GA, Forrester JS. Analysis of probability as an aid in the clinical diagnosis of coronary-artery disease. *N Engl J Med* 1979;**300**:1350–1358.

4. Pryor DB, Harrell FE Jr, Lee KL, Califf RM, Rosati RA. Estimating the likelihood of significant coronary artery disease. *Am J Med* 1983;**75**:771–780.

5. Genders TS, Steyerberg EW, Alkadhi H, Leschka S, Desbiolles L, Nieman K, Galema TW, Meijboom WB, Mollet NR, de Feyter PJ, Cademartiri F, Maffei E, Dewey M, Zimmermann E, Laule M, Pugliese F, Barbagallo R, Sinitsyn V, Bogaert J, Goetschalckx K, Schoepf UJ, Rowe GW, Schuijf JD, Bax JJ, de Graaf FR, Knuuti J, Kajander S, van Mieghem CA, Meijs MF, Cramer MJ, Gopalan D, Feuchtner G, Friedrich G, Krestin GP, Hunink MG, The CAD Consortium. A clinical prediction rule for the diagnosis of coronary artery disease: validation, updating, and extension. *Eur Heart J* 2011;**32**:1316–1330.

6. Bittencourt MS, Hulten E, Polonsky TS, Hoffman U, Nasir K, Abbara S, Di Carli M, Blankstein R. European Society of Cardiology-recommended coronary artery disease consortium pretest probability scores more accurately predict obstructive coronary disease and cardiovascular events than the Diamond and Forrester score: the Partners Registry. *Circulation* 2016;**134**:201–211.

7. Almeida J, Fonseca P, Dias T, Ladeiras-Lopes R, Bettencourt N, Ribeiro J, Gama V. Comparison of coronary artery disease consortium 1 and 2 scores and Duke clinical score to predict obstructive coronary disease by invasive coronary angiography. *Clin Cardiol* 2016;**39**:223–228.

8. Fordyce CB, Douglas PS, Roberts RS, Hoffmann U, Al-Khalidi HR, Patel MR, Granger CB, Kostis J, Mark DB, Lee KL, Udelson JE, for the Prospective Multicenter Imaging Study for Evaluation of Chest Pain (PROMISE) Investigators. Identification of patients with stable chest pain deriving minimal value from non-invasive testing: the PROMISE minimal-risk tool, A secondary analysis of a randomized clinical trial. *JAMA Cardiol* 2017;**2**:400–408.

9. Genders TS, Steyerberg EW, Hunink MG, Nieman K, Galema TW, Mollet NR, de Feyter PJ, Krestin GP, Alkadhi H, Leschka S, Desbiolles L, Meijs MF, Cramer MJ, Knuuti J, Kajander S, Bogaert J, Goetschalckx K, Cademartiri F, Maffei E, Martini C, Seitun S, Aldrovandi A, Wildermuth S, Stinn B, Fornaro J, Feuchtner G, De Zordo T, Auer T, Plank F, Friedrich G, Pugliese F, Petersen SE, Davies LC, Schoepf UJ, Rowe GW, van Mieghem CA, van Driessche L, Sinitsyn V, Gopalan D, Nikolaou K, Bamberg F, Cury RC, Battle J, Maurovich-Horvat P, Bartykowszki A, Merkely B, Becker D, Hadamitzky M, Hausleiter J, Dewey M, Zimmermann E, Laule M. Prediction model to estimate presence of coronary artery disease: retrospective pooled analysis of existing cohorts. *BMJ* 2012;**344**: e3485.

10. Christoffersen M, Tybjærg-Hansen A. Visible aging signs as risk markers for ischemic heart disease: epidemiology, pathogenesis and clinical implications. *Ageing Res Rev* 2016;**25**:24–41.

11. Christoffersen M, Frikke-Schmidt R, Schnohr P, Jensen GB, Nordestgaard BG, Tybjærg-Hansen A. Visible age-related signs and risk of ischemic heart disease in the general population a prospective cohort study. *Circulation* 2014;**129**:990–998.

12. Schnohr P, Lange P, Nyboe J, Appleyard M, Jensen G. Gray hair, baldness, and wrinkles in relation to myocardial infarction: the Copenhagen city heart study. *Am Heart J* 1995;**130**:1003–1010.

13. Ang M, Wong W, Park J, Wu R, Lavanya R, Zheng Y, Cajucom-Uy H, Tai ES, Wong TY. Corneal arcus is a sign of cardiovascular disease, even in low-risk persons. *Am J Ophthalmol* 2011;**152**:864–871.e1.

14. Wang Y, Mao LH, Jia EZ, Li ZY, Ding XQ, Ge PC, Liu Z, Zhu TB, Wang LS, Li CJ, Ma WZ, Yang ZJ. Relationship between diagonal earlobe creases and coronary artery disease as determined via angiography. *BMJ Open* 2016;**6**:e008558.

15. Gunn DA, Murray PG, Tomlin CC, Rexbye H, Christensen K, Mayes AE. Perceived age as a biomarker of ageing: a clinical methodology. *Biogerontology* 2008;**9**:357–364.

16. Kosilek RP, Frohner R, Würtz RP, Berr CM, Schopohl J, Reincke M, Schneider HJ. Diagnostic use of facial photo analysis software in endocrine and genetic disorders: review, current results and future perspectives. *Eur J Endocrinol* 2015;**173**:M39–M44.

17. Gurovich Y, Hanani Y, Bar O, Nadav G, Fleischer N, Gelbman D, Basel-Salmon L, Krawitz PM, Kamphausen SB, Zenker M, Bird LM, Gripp KW. Identifying facial phenotypes of genetic disorders using deep learning. *Nat Med* 2019;**25**:60–64.

18. Buderer NM. Statistical methodology: I. Incorporating the prevalence of disease into the sample size calculation for sensitivity and specificity. *Acad Emerg Med* 1996;**3**:895–900.

19. Stephen ID, Hiew V, Coetzee V, Tiddeman BP, Perrett DI. Facial shape analysis identifies valid cues to aspects of physiological health in Caucasian, Asian, and African populations. *Front Psychol* 2017;**8**:1883.

20. Coetzee V, Perrett DI, Stephen ID. Facial adiposity: a cue to health? *Perception* 2009;**38**:1700–1711.

21. Eric NR, Robert MH, Karen CS. Predicting adult health and mortality from adolescent facial characteristics in yearbook photographs. *Demography* 2009;**46**: 27–41.

22. Christensen K, Thinggaard M, McGue M, Rexbye H, Hjelmborg JV, Aviv A, Gunn D, van der Ouderaa F, Vaupel JW. Perceived age as clinically useful biomarker of ageing: cohort study. *BMJ* 2009;**339**:b5262.

23. Zhao C, Li GZ, Li F, Wang Z, Liu C. Qualitative and quantitative analysis for facial complexion in traditional Chinese medicine. *Biomed Res Int* 2014;**2014**:1–17.

24. Reeh J, Therming CB, Heitmann M, Højberg S, Sørum C, Bech J, Husum D, Dominguez H, Sehestedt T, Hermann T, Hansen KW, Simonsen L, Galatius S, Prescott E. Prediction of obstructive coronary artery disease and prognosis in patients with suspected stable angina. *Eur Heart J* 2019;**40**:1426–1435.

25. Miller JM, Rochitte CE, Dewey M, Arbab-Zadeh A, Niinuma H, Gottlieb I, Paul N, Clouse ME, Shapiro EP, Hoe J, Lardo AC, Bush DE, de Roos A, Cox C, Brinker J, Lima JAC. Diagnostic performance of coronary angiography by 64-row CT. *N Engl J Med* 2008;**359**:2324–2336.